

Wide & deep learning for spatial & intensity adaptive image restoration

Yadong Wang¹

Xiangzhi Bai^{1,2,3*}

¹Image Processing Center, Beihang University, Beijing, China

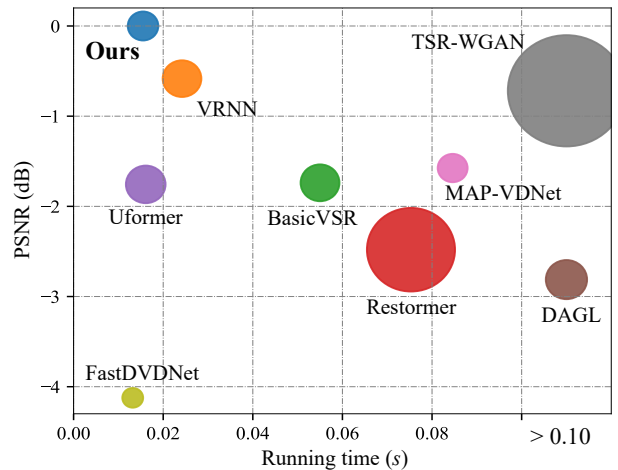
²State Key Laboratory of Virtual Reality Technology and Systems, Beihang University, Beijing, China

³Advanced Innovation Center for Biomedical Engineering, Beihang University, Beijing, China

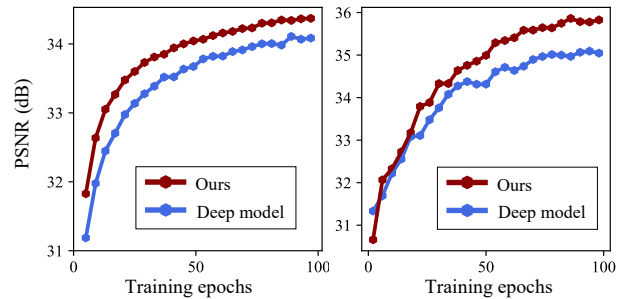
ydwang@outlook.com, jackybxz@buaa.edu.cn

Abstract

Most existing deep learning-based image restoration methods usually aim to remove degradation with uniform spatial distribution and constant intensity, making insufficient use of degradation prior knowledge. Here we bootstrap the deep neural networks to suppress complex image degradation whose intensity is spatially variable, through utilizing prior knowledge from degraded images. Specifically, we propose an ingenious and efficient multi-frame image restoration network (DparNet) with wide & deep architecture, which integrates degraded images and prior knowledge of degradation to reconstruct images with ideal clarity and stability. The degradation prior is directly learned from degraded images in form of key degradation parameter matrix, with no requirement of any off-site knowledge. The wide & deep architecture in DparNet enables the learned parameters to directly modulate the final restoring results, boosting spatial & intensity adaptive image restoration. We demonstrate the proposed method on two representative image restoration applications: image denoising and suppression of atmospheric turbulence effects in images. Two large datasets, containing 109,536 and 49,744 images respectively, were constructed to support our experiments. The experimental results show that our DparNet significantly outperform SoTA methods in restoration performance and network efficiency. More importantly, by utilizing the learned degradation parameters via wide & deep learning, we can improve the PSNR of image restoration by 0.6~1.1 dB with less than 2% increasing in model parameter numbers and computational complexity. Our work suggests that degraded images may hide key information of the degradation process, which can be utilized to boost spatial & intensity adaptive image restoration.



(a) Network efficiency comparison



(b) Training curves in image denoising and deturbulence

Figure 1: Wide & deep learning boosts efficient image restoration. (a) is drawn according to relative PSNR and average running time to restore a $256 \times 256 \times 3$ image for our method and SoTA restoration methods. Area of each circle in (a) is proportional to the number of model parameters. (b) shows the promotion of wide & deep learning on improving restoration performance.

*Corresponding author

1. Introduction

The imaging of natural scenes suffers from various types of image degradation, which can be caused by physical limitations of camera or by harsh imaging environments. For instance, electromagnetic interference from inside and outside camera causes noise in imaging results, which is particularly noticeable in dark scenes. When imaging at medium or long distance in hot weather, the disturbance of optical path caused by atmospheric turbulence leads to multiple forms of image degradation, including geometric distortion, blurring [16, 34], *etc.* These degradations severely degrade the quality of image or video, which affects subsequent imaging-based civilian or military applications such as security surveillance and visual navigation guidance.

Numerous attempts have been made to mitigate the negative effects of image degradation. Traditional methods rely on modelling degradation to approximate the inverse process and realise image restoration [9, 24]. In recent years, deep learning has freed researchers from complex modelling and optimisation, enabling establishment of end-to-end mapping from degraded image to restored image [13, 38, 27]. However, most existing deep learning-based methods focus only on addressing of image degradation with constant intensity and uniform spatial distribution [29, 12, 20, 36, 31]. These methods lack attention to intensity fluctuation and spatial distribution of degradation and adopt spatially consistent restoring strategies, which limits their ability to settle complex degradation. In addition, most existing methods make insufficient use of degradation prior knowledge when performing restoration, leading to low efficiency and poor interpretability. There lacks methods capable of handling spatially inhomogeneous, intensity-varying degradation, which is of great challenge and research value.

Notably, degradation information in imaging process determines the manifestation, spatial distribution and intensity change of image degradation, which can provide strong prior knowledge for image restoration. The difficulty of obtaining prior information has been puzzling the field of image restoration, forcing most deep learning methods to adopt a data-driven blind restoration strategy. Nevertheless, we assume that the degradation prior is just hidden in degraded images, and it can be learned in a parametrised manner to guide neural networks in image restoration.

In this paper, we propose an efficient framework to perform intensity & spatially adaptive multi-frame image restoration. In specific, we first learn key degradation parameters from degraded images through parameter prediction network with a simple encoder-decoder architecture. The learned parameters and degraded sequences are fed together into our degradation parameter assisted restoration network (DparNet in Figure 2). The proposed DparNet adopts a wide & deep architecture, inspired by Google's

wide & deep learning for recommender systems [5]. The deep model performs in-depth down-sampling encoding on the input degraded sequence and produce high quality restored sequence end-to-end. The wide model, with a shallow encoding depth, wide feature resolution and small number of model parameters, integrates both the learned degradation parameters and degraded image sequence. The deep and wide models are implemented in parallel, with final restoring result being a fusion of the outputs from these two sub-models. With the architecture of wide & deep models, DparNet makes full use of learned degradation parameters to guide the network in suppressing degradation varies in space and intensity, improving restoration performance remarkably with negligible increase in model size and computational complexity.

We demonstrate our method on two representative image restoration applications: image denoising and suppression of atmospheric turbulence degradation in images (denoted as image deturbulence). We constructed two large datasets, containing 109,536 and 49,744 images respectively, where degradation varies in intensity and spatial distribution. Experimental results show that our DparNet can effectively suppress degradation with spatial and intensity variations, and significantly outperform SoTA restoration methods. In addition, our method has been rationally and ingeniously designed to achieve particularly high network efficiency, *i.e.*, achieving excellent restoration performance with high processing speed, as shown in Figure 1 (a). More importantly, utilization of degradation prior by wide & deep learning greatly enhances restoration performance, as shown in training curves illustrated by Figure 1 (b). Quantitative results of the ablation study show that PSNR for image denoising and deturbulence is improved by 0.6 and 1.1 dB respectively via wide & deep learning, while the model size and computational complexity increase by less than 2%.

Overall, the main contributions can be summarised as:

1. New insight of learning degradation prior from degraded images to promote image restoration is explored, filling the gap in research of spatial & intensity adaptive image restoration.
2. We propose a novel multi-frame image restoration network (DparNet), which exploits learned degradation parameters to efficiently boost image restoration through a wide & deep architecture.
3. Large datasets for image denoising and deturbulence were constructed, where degradation changes in space and intensity, to facilitate the research community.
4. Extensive experiments demonstrate the promotion to restoration performance from utilization of degradation prior, and our DparNet outperforms SoTA methods in restoration performance and network efficiency.

2. Related work

2.1. Image restoration

Image restoration, an important fundamental technique in computer vision, aims to use single or multiple degraded images with prior knowledge to obtain the desired image [2]. Compared with improving imaging hardware to avoid degradation [22], restoring ideal image from degraded image is a more cost-effective choice. Traditional image restoration methods model the degradation process and then iterate through mathematical optimisations to approximate the ideal image [9, 8]. Accurate modelling the degradation is crucial for restoring ideal images, which limits the application value of traditional restoration methods. Deep learning enables the building of end-to-end mapping from degraded image to restored image. In recent years, deep learning-based image restoration methods have shown outstanding performance [12, 20, 36, 31]. However, most existing deep learning-based methods focus only on degradation with constant intensity and uniform spatial distribution, such as random noise with fixed intensity level [31, 28, 30]. Although one research attempt to locate the spatial distribution of degradation to guide spatially adaptive image restoration [21], it still lacks consideration of degradation intensity change and the utilization of degradation prior knowledge. In this paper we aim to make full use of degradation prior hidden in degraded images to fully suppress degradation varies in space and intensity. We demonstrate our method on two representative image restoration tasks: image denoising and deturbulence. Next, we will briefly introduce the representative methods of these two tasks.

2.2. Image denoising

Image denoising is a classic image restoration task with a long research history. An early image denoising technique integrates similar pixel information in neighbouring fields through non-linear filtering to reduce image noise [26]. Later traditional methods achieve image denoising via sparse representation of image or by means of regional self-similarity [9, 8, 6]. The popularity of deep learning has greatly promoted the performance of image denoising [10, 29, 28]. As end-to-end methods rely on large amounts of training data rather than degradation modelling, some recent research has been devoted to developing general methods that can address wide types of image degradation, and these methods have become SoTA methods for image denoising [36, 33, 31]. However, the above deep learning-based methods are content to suppress spatially uniform noise with constant intensity level and lack the ability to settle complex noise varies in intensity and space.

2.3. Image deturbulence

Unlike image degradation due to physical limitations of camera hardware, the atmospheric turbulence degradation on images is primarily caused by physical properties of imaging medium [12]. Atmospheric turbulence causes irregular fluctuations in refractive index of atmosphere, leading to bending and dissipation of optical path, which results in strong random geometric distortions and blurring on imaging data [18, 16, 7]. To alleviate atmospheric turbulence degradation in infrared or visible light image, traditional methods adopt multi-frame registration-fusion and deconvolution techniques to realise image deturbulence [11, 1, 4, 17]. The difficulty of collecting paired data has limited the research of deep learning-based image deturbulence methods. One recent study constructed datasets through algorithm and heat source simulations, achieving good results on image deturbulence [12].

3. The proposed method

3.1. Problem formulation and motivation

In general, the degradation process for image can be formulated as:

$$D = H(C) + N, \quad (1)$$

where D , C and N are degraded image, clean image and additional noise. $H(\cdot)$ represents degradation function. Assuming that $H(\cdot)$ contains noise degradation, then N in formula (1) can be omitted. When using deep neural network (DNN) to solve the inverse process of formula (1), the optimization of DNN can be formulated as [31]:

$$W^* = \arg \min_W \|\text{DNN}(D; W) - C\|, \quad (2a)$$

$$\hat{C} = \text{DNN}(D; W^*), \quad (2b)$$

where $\text{DNN}(\cdot; W)$ represents a deep neural network with parameter W . The trained DNN can approximate H^{-1} to achieve image restoration.

However, when intensity and spatial distribution of degradation change, the effectiveness of a trained DNN decreases. The reason is that a fixed DNN cannot approximate the reverse process of a dynamically changing H . Considering the variability of degradation, formula (1) should be modified to:

$$D = H(C; P), \quad (3)$$

where P denotes key degradation parameters that characterise degradation. P represent different parameters in different degradation. For instance, P are noise intensity level σ_n and turbulence intensity C_n^2 in noise degradation and atmospheric turbulence degradation, respectively. In fact, P could be any parameter that dominates degradation. Considering the spatial distribution of degradation, P is supposed to be a two-dimensional matrix that

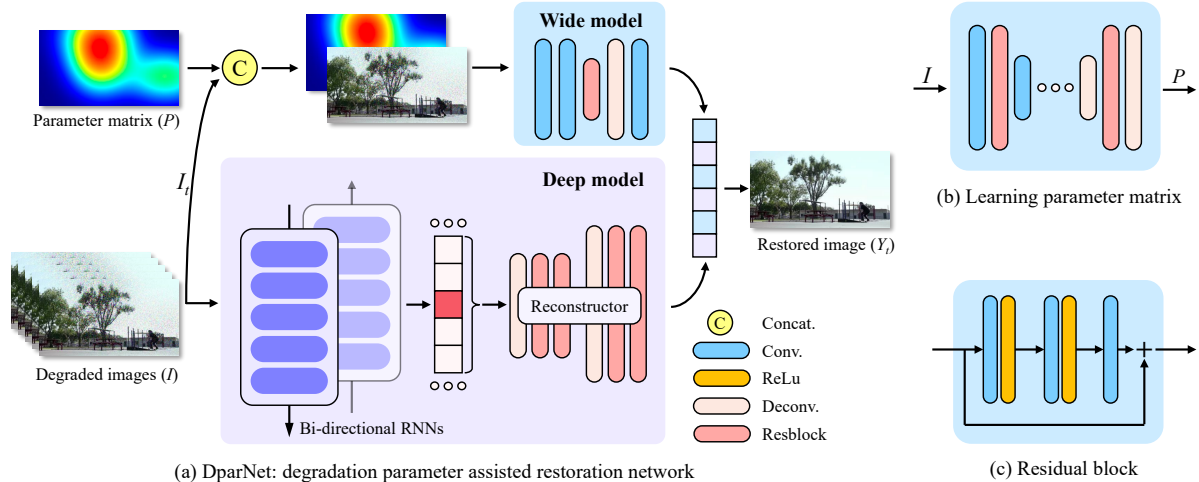


Figure 2: Overall structure of the proposed method. The learned degradation parameter matrix (P) is integrated with degraded images (I) via our DparNet in (a), which adopts a wide & deep architecture, to generate restored images (Y).

matches the degraded image spatially. Based on formula (3), an easy-to-think improvement to formula (2) is to replace $\text{DNN}(D; W)$ with $\text{DNN}(D, P; W)$, as follows:

$$W^* = \arg \min_W \|\text{DNN}(D, P; W) - C\|, \quad (4a)$$

$$\hat{C} = \text{DNN}(D, P; W^*). \quad (4b)$$

Although the improvement in formula (4) could be helpful, the direct use of prior knowledge as additional input may invalidate the prior by being submerged in dense features [5]. In fact, simple architecture enables prior knowledge to directly affect the final result [23]. Introducing degradation prior through simple architecture is a more potential strategy. Based on this motivation, we give the restoration paradigm of this paper:

$$\hat{C} = \text{Merge}(\text{DM}(D; W_D), \text{WM}(D, P; W_W)), \quad (5)$$

where DM denote a deep model, i.e., DNN mentioned above, WM is a wide model with simple architecture and wide feature resolution. Through the concise and effective paradigm in formula (5), we not only retain the powerful non-linear mapping ability of the deep model, but also allows prior knowledge to modulate the final restoration result without hindrance.

The question left to be addressed is the acquisition of parameter matrix P . Notably, since the manifestation, spatial distribution and intensity variation of degradation are highly related to characteristics of key degradation parameters, the possibility of revealing degradation parameter matrix directly from degraded images exists, which has potential to provide an easily-available and powerful prior for image restoration. Based on the above and motivations, we have developed the framework of this paper.

3.2. Overall workflow

We propose an efficient and ingenious framework for spatial & intensity adaptive image restoration (Figure 2), whose overall workflow can be outlined in four steps. Firstly, a parameter prediction network consisting of several convolutional and deconvolutional layers is used to learn the numerical matrix of key degradation parameters, such as noise intensity level σ_n or turbulence intensity C_n^2 , from the input degraded image sequence. Secondly, the degraded images and learned parameter matrix are fed into the proposed degradation parameter assisted restoration network (DparNet) for parallel processing. Wide & deep architecture in DparNet enables learned parameter matrix to act directly on the reconstruction results as a degradation prior rather than being submerged in dense image features. Thirdly, the results of wide & deep models are merged to obtain the final restoration results. Finally in test phase, the only required input for whole framework is the degraded image sequence, while output includes degradation parameter matrix and restored image sequence.

3.3. The proposed DparNet

Architecture of the proposed DparNet is illustrated in Figure 2 (a). DparNet adopts a wide & deep architecture. The deep model is an efficient multi-frame image restoration network that enables end-to-end mapping from degraded sequence to restored sequence. The deep model performs multi-layer downsampling and deep encoding of the degraded sequence, and then reconstructs restored sequence from the extracted image features. In specific, the input degraded sequence (I) is first encoded into dense image features via a feature extractor implemented by a bi-

directional recurrent neural network (BRNN). The BRNN we used, streamlined from the version proposed by Wang *et al.*, has been demonstrated to be effective for wide types of multi-frame image restoration [31]. We streamlined the BRNN from Wang *et al.* by reducing in half the number of residual dense blocks [37] to achieve high network efficiency. The extracted features, denoted as F , are decoded by a reconstructor (RC) composed of several residual blocks and transposed convolutional layers. Each restored target frame (Y_t) is reconstructed by fusing its feature map and the feature maps of four neighbouring frames. The workflow of deep model can be formulated as follows:

$$\dots, F_t, F_{t+1}, \dots = \text{BRNN}(\dots, I_t, I_{t+1}, \dots), \quad (6a)$$

$$Y_t = \text{RC}(\text{Cat}(F_{t-2}, F_{t-1}, F_t, F_{t+1}, F_{t+2})), \quad (6b)$$

where $\text{Cat}(\cdot)$ is the operation of concatenation.

Another aspect, the degraded target frame, concatenated with the learned parameter matrix, are fed into the wide model. Our wide model containing only three convolutional layers, one deconvolutional layer and one residual block, as shown in Figure 2 (a). The number of parameters for wide model is approximately 1% of that for deep model, which aims to introduce the assistance of degradation prior without bringing perceptible additional computational burden. The image features maintain a “wide” resolution in wide model, different from deep downsampling and encoding in deep model. The shallow encoding level and wide resolution in wide model enable parameter matrix to directly modulate the final result. The restored image is obtained by merging the outputs of wide and deep model, as follows:

$$\dots, Y_t^1, Y_{t+1}^1, \dots = \text{DM}(\dots, I_t, I_{t+1}, \dots), \quad (7a)$$

$$Y_t^2 = \text{WM}(\text{Cat}(I_t, P)), \quad (7b)$$

$$Y_t = \text{Conv}_{1 \times 1}(\text{Cat}(Y_t^1, Y_t^2)), \quad (7c)$$

where $\text{DM}(\cdot)$ and $\text{WM}(\cdot)$ denote the processing by deep and wide models, $\text{Conv}_{1 \times 1}(\cdot)$ means adjusting the channels via a convolutional layer with kernel size of 1×1 . Each reconstructed frame is then concatenated in temporal order to obtain the restored sequence.

Overall, our framework is developed based on a simple but non-trivial insight: degradation information hidden in degraded images can be revealed and used as prior knowledge to facilitate image restoration. In order to avoid the degraded parameter matrix being submerged by dense image features extracted by deep model, we adopt a wide & deep architecture to make parameter matrix directly affect the final restoration result. Based on the above designs, our DparNet has the potential to achieve efficient spatial & intensity adaptive image restoration.

3.4. Implementation details

Our DparNet was trained with a loss function composed of pixel loss and perceptual loss [15], as follows:

$$L = \alpha_1 L_{\text{pixel}} + \alpha_2 L_{\text{perceptual}}, \quad (8)$$

where L denotes the loss function, α_1 and α_2 are taken as 1 and 0.05 respectively in this work. The pixel loss was calculated through the \mathcal{L}_1 distance between restored image and ground truth. The perceptual loss was obtained by feeding the restored image and ground truth into a pre-trained feature extraction model (VGG19 [25]) and calculating \mathcal{L}_1 distance between the outputs. In addition, the parameter prediction network was trained via the \mathcal{L}_1 distance between the predicted parameter matrix and ground truth.

During the training, we randomly cropped the image into 256×256 patches and randomly flipped the input image horizontally or/and vertically. Adam [14] optimizer was adopted to train our model for 100 epochs with the learning rate as 0.0001. Our experiments were conducted on a platform with Windows 10 system and 2 NVIDIA RTX 3090-Ti graphics cards. All of our data and code will be released publicly to facilitate the research community.

4. Experimental results

4.1. Dataset construction and evaluation manners

We conducted experiments on two representative restoration applications: image denoising and deturbulence. Datasets for these two tasks, with degradation changes in space and intensity, were constructed for training and evaluating the proposed method and comparison methods. The denoising dataset was constructed on the basis of Vimeo-90K dataset [35]. Additive random noise with complex random spatial distribution and random intensity level ($0 \leq \sigma_n \leq 100$) was added to clear images to obtain noise-degraded images as network inputs. The denoising dataset contains 7,824 pairs of degraded-clean sequences with a total of 109,536 images with resolution of $256 \times 448 \times 3$. The frame length of denoising dataset is 7, according to the pre-division of Vimeo-90K dataset. The 20% of data was used for test, and the rest was used for training and validation.

Another aspect, our deturbulence dataset was constructed through outdoor photography using a FLIR A615 thermal infrared camera. We simulated the atmospheric turbulence degradation (geometric distortion and blurring) with complex random spatial distribution and random intensity ($0 \leq C_n^2 \leq 6 \times 10^{-12}$) on clear images using simulation algorithm from Jin *et al.* [12]. The training set contains 1,302 pairs of degraded-clean sequences with a total of 39,060 images. The test set contains 40 pairs of degraded-clean sequences with a total of 10,684 images. The training sequence has been standardised to 15 frames, while the

Methods	PSNR (\uparrow)	SSIM (\uparrow)	NRMSE (\downarrow)	VI (\downarrow)
FastDVDNet [29]	29.2781	0.8169	0.1821	9.3020
MAP-VDNet [28]	31.8261	0.8899	0.0770	8.1362
BasicVSR [3]	32.9615	0.9028	0.0693	7.9442
DAGL [20]	31.2747	0.8815	0.0820	8.3634
Uformer [33]	31.6437	0.8792	0.0799	8.2328
Restormer [36]	32.2736	0.8926	0.0736	7.9846
VRNN [31]	32.8921	0.9052	0.0691	7.7636
Ours	33.4012	0.9143	0.0652	7.7184

Table 1: Quantitative comparison of image denoising. Symbol (\uparrow) indicates that higher values have better performance, while (\downarrow) is the opposite. The best results are **in bold**.

frame length of test sequence varies from tens to hundreds. The resolution of our deturbulence data is 480×640 .

Quantitative and qualitative assessments have been conducted to evaluate the restoration performance. Adopted quantitative metrics include Peak Signal to Noise Ratio (PSNR), Structural Similarity (SSIM) [32], Normalized Root Mean Square Error (NRMSE), and Variation of Information (VI) [19]. Qualitative assessments are conducted through the visualisation of restoring results. In addition to evaluating the restoration performance, we compare network efficiency of the proposed model and comparison models by counting the number of model parameters, the average FLOPs and running time. All the comparison methods adopted the same data augmentation and training strategies as the proposed method.

4.2. Performance on image denoising

We compare the proposed DparNet with 7 SoTA image/video denoising or restoration methods based on deep learning, including FastDVDNet [29], MAP-VDNet [28], BasicVSR [3], DAGL [20], Uformer [33], Restormer [36], and VRNN [31]. Quantitative metrics for evaluating restoration performance of the proposed method and comparison methods are reported in Table 1. The proposed method achieves the best results in all four image quality assessment metrics, with PSNR of our method being 0.44 to 4.12 dB higher than that of the comparison methods. From the subjective visual comparison shown in Figure 3, the proposed method effectively suppresses the spatial & intensity varying noise in input image and achieves the restoration results closest to ground truth. For areas with weak noise intensity, the restoration results of most comparison methods are acceptable, such as the restoration of pedestrian objects in Figure 3. However, when noise intensity increases, the restoration performance of comparison methods decreases. In the second comparison of Figure 3, almost all comparison methods fail to restore textures of the building, only our method can suppress strong noise and restore image details well. The above results show that the proposed method

Methods	PSNR (\uparrow)	SSIM (\uparrow)	NRMSE (\downarrow)	VI (\downarrow)
SGF [17]	27.8677	0.8562	0.0766	8.8624
CLEAR [1]	32.2483	0.8999	0.0475	7.5707
BasicVSR [3]	31.1472	0.8719	0.0553	7.3905
TSR-WGAN [12]	33.2667	0.9065	0.0427	7.0831
DAGL [20]	30.4874	0.8427	0.0583	8.1927
Restormer [36]	30.1516	0.8384	0.0599	8.1288
VRNN [31]	33.3376	0.9081	0.0421	7.0141
Ours	33.9853	0.9195	0.0397	6.7744

Table 2: Quantitative comparison of image deturbulence.

Models	Params	FLOPs	Time (s)	PSNR
Ours	3.1496	3.4924	0.0155	0
VRNN [31]	5.0357	4.6890	0.0242	-0.5839
TSR-WGAN [12]	46.2849	31.2422	0.1793	-0.7186
MAP-VDNet [28]	3.0142	29.1712	0.0846	-1.5751
BasicVSR [3]	4.0756	27.6860	0.0550	-1.7389
Uformer [33]	5.2919	1.0684	0.0161	-1.7563
Restormer [36]	26.1266	14.0990	0.0753	-2.4807
DAGL [20]	5.7297	27.3386	0.5449	-2.8122
FastDVDNet [29]	1.4598	4.3679	0.0132	-4.1231

Table 3: Comparison of network efficiency. Params are number of model parameters divided by 10^6 , FLOPs are average floating point operations, divided by 10^{10} , to process a frame with shape of $256 \times 256 \times 3$. Time (s) is the average running time for a model to process a frame, with shape of $256 \times 256 \times 3$, in 100 testing rounds on a RTX 3090-Ti graphics card. If a model has been used in multiple tasks, the average indicator is reported.

outperforms SoTA methods objectively and subjectively in image denoising.

4.3. Performance on image deturbulence

We compare the proposed DparNet with 7 image/video restoration or deturbulence methods, including 2 traditional registration-fusion-based methods: SGF [17] and CLEAR [1], along with 5 SoTA deep learning-based methods: BasicVSR [3], TSR-WGAN [12], DAGL [20], Restormer [36], and VRNN [31]. Quantitative metrics are reported in Table 2. The proposed method achieves the best results in all four image quality assessment metrics, with PSNR of our method being 0.65 to 6.12 dB higher than that of comparison methods. Another aspect, from the subjective visual comparison shown in Figure 4, the proposed method effectively suppresses the spatial & intensity varying turbulence degradation in the input image, including geometric distortion and blurring, obtaining the clearest, closest-to-ground truth restoring results. In the first comparison with relatively weak degradation intensity, VRNN, TSR-WGAN and our method achieve acceptable restoration results, among which our result is the best. Advantages of the proposed method become more apparent when the intensity of degra-

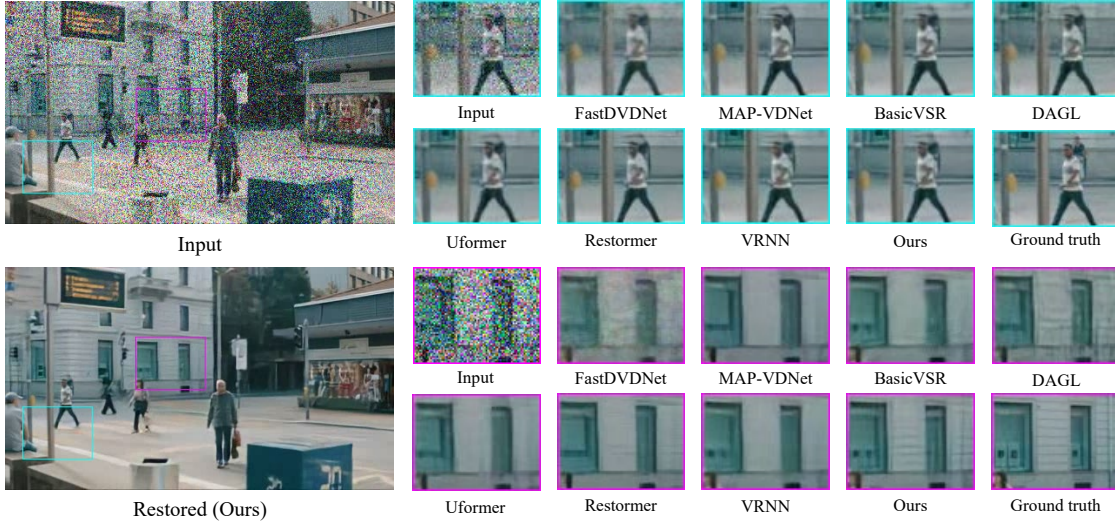


Figure 3: Visual comparison of image denoising.

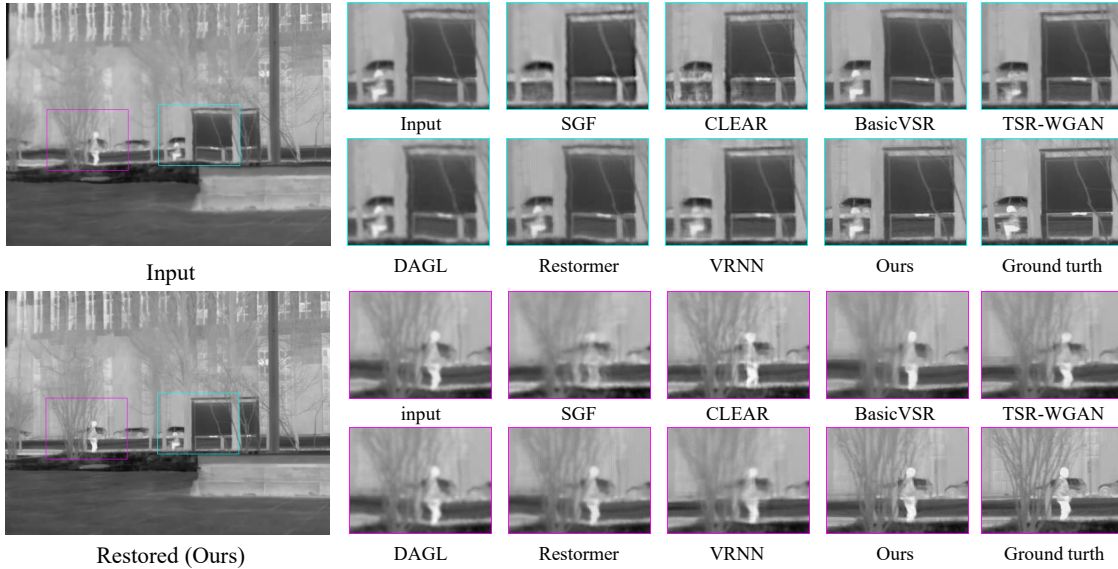


Figure 4: Visual comparison of image deturbulence.

dation increases, as shown in the second comparison of 4. Another aspect, although traditional deturbulence methods can restore the static background, they destroy the moving target (see SGF and CLEAR restoring results for pedestrian and cyclist). Further, we visualise the stability of sequences by arranging one column of pixels in temporal order. The comparison for deep learning-based methods are shown in Figure 5. The proposed method effectively suppresses the random geometric distortion in input sequence and obtains the most stable restoration results against comparison methods. The above results show that the proposed method out-

performs SoTA methods objectively and subjectively in image deturbulence. Notably, since the turbulence degradation is more complex than noise, the great advantages of the proposed method in image deturbulence show its great potential to settle complex degradation.

4.4. Network efficiency analysis

The rational and ingenious structural design make the proposed method highly efficient, i.e., our model achieves good performance with low model complexity. Table 3 reports the comparison of network efficiency between the

Model	P	W&D	Params	FLOPs	Time (s)	PSNR (\uparrow)	SSIM (\uparrow)	NRMSE (\downarrow)	VI (\downarrow)
Variant-1	\times	\times	3.1074	3.4302	0.0152	32.7923/32.8944	0.9082/0.9121	0.0675/0.0442	7.8012/6.9491
Variant-2	\checkmark	\times	3.1082	3.4399	0.0153	32.7881/33.0195	0.8996/0.9050	0.0706/0.0438	7.8024/7.1154
Variant-3	\times	\checkmark	3.1496	3.4924	0.0155	32.8699/33.3579	0.9120/0.9101	0.0702/0.0424	7.8702/6.9992
Ours	\checkmark	\checkmark	3.1496	3.4924	0.0155	33.4012/33.9853	0.9143/0.9195	0.0652/0.0397	7.7184/6.7744

Table 4: Results of ablation study. P denotes the degradation parameter matrix, “W&D” denotes wide & deep learning, “A/B” indicates that the metrics for denoising and deturbulence are A and B, respectively.

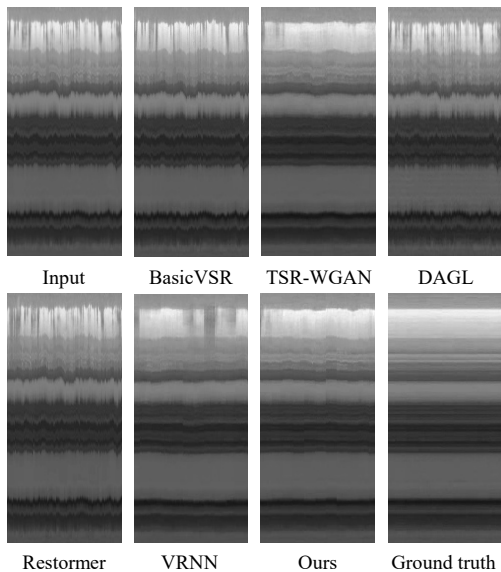


Figure 5: Stability comparison of image sequences.

proposed method and all deep learning-based comparison methods. Model parameters, average floating point operations (FLOPs), running time and relative PSNR are counted. It can be seen that the proposed model has the best restoration performance. Meanwhile, our model outperform most comparison models in model parameters, FLOPs, and running time, only slightly inferior than some methods whose restoration performance is noticeably weaker than our model, such as FastDVDNet. Figure 1 (a), plotted based on model parameters, running times and relative PSNR, visually demonstrates the advantages of our method in network efficiency.

4.5. Ablation study

In ablation study, we validate the effectiveness of wide & deep learning and utilization of degradation prior to boost image restoration, as shown in Table 4. We have made several variants of the proposed method. Variant-1 indicates using our deep model without parameter matrix assistance. Variant-2 indicates using deep model with parameter matrix as an additional input channel. Variant-3 uses the same wide & deep models as ours, but the parameter matrix is

replaced by a matrix in which all elements are equal to 1.

The results of variant-2 indicate that directly using learned parameter matrix as additional input into the deep model does not result in a significant performance improvement, which coincides with our assumption. Meanwhile, results of variant-3 show that using wide & deep architecture, without the assistance of degradation parameter matrix, has improvement in some restoration metrics, such as PSNR. However, gains of two variants mentioned above are weak compared to the facilitation brought by utilizing parameter matrix through wide & deep learning. Our method improves PSNR by 0.61 and 1.09 dB in image denoising and deturbulence, respectively, with less than 2% increasing in model parameter numbers and computational complexity. Further, the training curves in Figure 1 (b) clearly show that utilizing parameter matrix through wide & deep learning significantly improve restoration performance. Notably, degradation parameter assistance are more powerful in the task of image deturbulence than in denoising. Given the diverse and stochastic nature of atmospheric turbulence degradation, this preference suggests that our framework is particularly competent to settle complex image degradation.

5. Conclusions

In this paper, we bootstrap deep neural networks to achieve spatial & intensity adaptive image restoration by utilization degradation prior through wide & deep learning. Two large datasets for image denoising and deturbulence were constructed to conduct extensive experiments. The experimental results show that our method achieves excellent restoration performance with very low computational complexity. More importantly, utilizing degradation parameter matrix via wide & deep learning significantly improves the restoration performance, while the increased computational burden is negligible. Overall, we provide a SoTA approach for multi-frame image restoration and fills the gap in research of spatial & intensity adaptive image restoration.

References

- [1] Nantheera Anantrasirichai, Alin Achim, Nick G Kingsbury, and David R Bull. Atmospheric turbulence mitigation using complex wavelet-based fusion. *IEEE Transactions on Image Processing*, 22(6):2398–2408, 2013. 3, 6

- [2] Mark R Banham and Aggelos K Katsaggelos. Digital image restoration. *IEEE Signal Processing Magazine*, 14(2):24–41, 1997. 3
- [3] Kelvin CK Chan, Xintao Wang, Ke Yu, Chao Dong, and Chen Change Loy. Basicvsr: The search for essential components in video super-resolution and beyond. In *Proceedings of the IEEE/CVF Conference on Computer Vision and Pattern Recognition*, pages 4947–4956, 2021. 6
- [4] Stanley H Chan, Ramsin Khoshabeh, Kristofor B Gibson, Philip E Gill, and Truong Q Nguyen. An augmented lagrangian method for total variation video restoration. *IEEE Transactions on Image Processing*, 20(11):3097–3111, 2011. 3
- [5] Heng-Tze Cheng, Levent Koc, Jeremiah Harmsen, Tal Shaked, Tushar Chandra, Hrishi Aradhye, Glen Anderson, Greg Corrado, Wei Chai, Mustafa Ispir, et al. Wide & deep learning for recommender systems. In *Proceedings of the 1st Workshop on Deep Learning for Recommender Systems*, pages 7–10, 2016. 2, 4
- [6] Kostadin Dabov, Alessandro Foi, Vladimir Katkovnik, and Karen Egiazarian. Image denoising by sparse 3-d transform-domain collaborative filtering. *IEEE Transactions on Image Processing*, 16(8):2080–2095, 2007. 3
- [7] Stefan Dancu, Laurent Ibos, Yves Candau, and Simone Mattei. Improvement of building wall surface temperature measurements by infrared thermography. *Infrared Physics & Technology*, 46(6):451–467, 2005. 3
- [8] Weisheng Dong, Lei Zhang, Guangming Shi, and Xin Li. Nonlocally centralized sparse representation for image restoration. *IEEE Transactions on Image Processing*, 22(4):1620–1630, 2012. 3
- [9] Michael Elad and Michal Aharon. Image denoising via sparse and redundant representations over learned dictionaries. *IEEE Transactions on Image Processing*, 15(12):3736–3745, 2006. 2, 3
- [10] Shi Guo, Zifei Yan, Kai Zhang, Wangmeng Zuo, and Lei Zhang. Toward convolutional blind denoising of real photographs. In *Proceedings of the IEEE/CVF Conference on Computer Vision and Pattern Recognition*, pages 1712–1722, 2019. 3
- [11] Michael Hirsch, Suvrit Sra, Bernhard Schölkopf, and Stefan Harmeling. Efficient filter flow for space-variant multiframe blind deconvolution. In *Proceedings of the IEEE/CVF Conference on Computer Vision and Pattern Recognition*, pages 607–614, 2010. 3
- [12] Darui Jin, Ying Chen, Yi Lu, Junzhang Chen, Peng Wang, Zichao Liu, Sheng Guo, and Xiangzhi Bai. Neutralizing the impact of atmospheric turbulence on complex scene imaging via deep learning. *Nature Machine Intelligence*, 3(10):876–884, 2021. 2, 3, 5, 6
- [13] T. H. Kim, K. M. Lee, B. Schölkopf, and M. Hirsch. Online video deblurring via dynamic temporal blending network. In *Proceedings of the IEEE/CVF International Conference on Computer Vision*, pages 4058–4067, 2017. 2
- [14] Diederik P Kingma and Jimmy Ba. Adam: A method for stochastic optimization. *arXiv preprint arXiv:1412.6980*, 2014. 5
- [15] Christian Ledig, Lucas Theis, Ferenc Huszár, Jose Caballero, Andrew Cunningham, Alejandro Acosta, Andrew Aitken, Alykhan Tejani, Johannes Totz, Zehan Wang, et al. Photo-realistic single image super-resolution using a generative adversarial network. In *Proceedings of the IEEE/CVF Conference on Computer Vision and Pattern Recognition*, pages 4681–4690, 2017. 5
- [16] Detlef Lohse and Ke-Qing Xia. Small-scale properties of turbulent rayleigh-bénard convection. *Annual Review of Fluid Mechanics*, 42:335–364, 2010. 2, 3
- [17] Yifei Lou, Sung Ha Kang, Stefano Soatto, and Andrea L Bertozzi. Video stabilization of atmospheric turbulence distortion. *Inverse Problems & Imaging*, 7(3):839, 2013. 3, 6
- [18] ECS Megaw. Scattering of electromagnetic waves by atmospheric turbulence: Stellar scintillation and the spectrum of turbulence in the free atmosphere. *Nature*, 166(4235):1100–1101, 1950. 3
- [19] Marina Meilă. Comparing clusterings—an information based distance. *Journal of Multivariate Analysis*, 98(5):873–895, 2007. 6
- [20] Chong Mou, Jian Zhang, and Zhuoyuan Wu. Dynamic attentive graph learning for image restoration. In *Proceedings of the IEEE/CVF International Conference on Computer Vision*, pages 4328–4337, 2021. 2, 3, 6
- [21] Kuldeep Purohit, Maitreya Suin, AN Rajagopalan, and Vishnu Naresh Boddeti. Spatially-adaptive image restoration using distortion-guided networks. In *Proceedings of the IEEE/CVF International Conference on Computer Vision*, pages 2309–2319, 2021. 3
- [22] François Rigaut and Benoit Neichel. Multiconjugate adaptive optics for astronomy. *Annual Review of Astronomy and Astrophysics*, 56:277–314, 2018. 3
- [23] Xiang-Rong Sheng, Liqin Zhao, Guorui Zhou, Xinyao Ding, Binding Dai, Qiang Luo, Siran Yang, Jingshan Lv, Chi Zhang, Hongbo Deng, et al. One model to serve all: Star topology adaptive recommender for multi-domain ctr prediction. In *Proceedings of the 30th ACM International Conference on Information & Knowledge Management*, pages 4104–4113, 2021. 4
- [24] Masao Shimizu, Shin Yoshimura, Masayuki Tanaka, and Masatoshi Okutomi. Super-resolution from image sequence under influence of hot-air optical turbulence. In *Proceedings of the IEEE/CVF Conference on Computer Vision and Pattern Recognition*, pages 1–8, 2008. 2
- [25] Karen Simonyan and Andrew Zisserman. Very deep convolutional networks for large-scale image recognition. *arXiv preprint arXiv:1409.1556*, 2014. 5
- [26] Stephen M Smith and J Michael Brady. Susan—a new approach to low level image processing. *International Journal of Computer Vision*, 23(1):45–78, 1997. 3
- [27] S. Su, M. Delbracio, J. Wang, G. Sapiro, W. Heidrich, and O. Wang. Deep video deblurring for hand-held cameras. In *Proceedings of the IEEE/CVF Conference on Computer Vision and Pattern Recognition*, pages 237–246, 2017. 2
- [28] Lu Sun, Weisheng Dong, Xin Li, Jinjian Wu, Leida Li, and Guangming Shi. Deep maximum a posterior estimator for

- video denoising. *International Journal of Computer Vision*, 129:2827–2845, 2021. 3, 6
- [29] Matias Tassano, Julie Delon, and Thomas Veit. Fastdvdnet: Towards real-time deep video denoising without flow estimation. In *Proceedings of the IEEE/CVF Conference on Computer Vision and Pattern Recognition*, pages 1354–1363, 2020. 2, 3, 6
- [30] Gregory Vaksman, Michael Elad, and Peyman Milanfar. Patch craft: Video denoising by deep modeling and patch matching. In *Proceedings of the IEEE/CVF International Conference on Computer Vision*, pages 2157–2166, 2021. 3
- [31] Yadong Wang and Xiangzhi Bai. Versatile recurrent neural network for wide types of video restoration. *Pattern Recognition*, page 109360, 2023. 2, 3, 5, 6
- [32] Zhou Wang, Alan C Bovik, Hamid R Sheikh, and Eero P Simoncelli. Image quality assessment: from error visibility to structural similarity. *IEEE Transactions on Image Processing*, 13(4):600–612, 2004. 6
- [33] Zhendong Wang, Xiaodong Cun, Jianmin Bao, Wengang Zhou, Jianzhuang Liu, and Houqiang Li. Uformer: A general u-shaped transformer for image restoration. In *Proceedings of the IEEE/CVF Conference on Computer Vision and Pattern Recognition*, pages 17683–17693, June 2022. 3, 6
- [34] Bindang Xue, Lei Cao, Linyan Cui, Xiangzhi Bai, Xiaoguang Cao, and Fugen Zhou. Analysis of non-kolmogorov weak turbulence effects on infrared imaging by atmospheric turbulence mtf. *Optics Communications*, 300:114–118, 2013. 2
- [35] Tianfan Xue, Baian Chen, Jiajun Wu, Donglai Wei, and William T Freeman. Video enhancement with task-oriented flow. *International Journal of Computer Vision*, 127(8):1106–1125, 2019. 5
- [36] Syed Waqas Zamir, Aditya Arora, Salman Khan, Munawar Hayat, Fahad Shahbaz Khan, and Ming-Hsuan Yang. Restormer: Efficient transformer for high-resolution image restoration. In *Proceedings of the IEEE/CVF Conference on Computer Vision and Pattern Recognition*, pages 5728–5739, 2022. 2, 3, 6
- [37] Yulun Zhang, Yapeng Tian, Yu Kong, Bineng Zhong, and Yun Fu. Residual dense network for image restoration. *IEEE Transactions on Pattern Analysis and Machine Intelligence*, 43(7):2480–2495, 2020. 5
- [38] S. Zhou, J. Zhang, J. Pan, W. Zuo, H. Xie, and J. Ren. Spatio-temporal filter adaptive network for video deblurring. In *Proceedings of the IEEE/CVF International Conference on Computer Vision*, pages 2482–2491, 2019. 2